What Drives Drilling Up and Prices Down?

A Structural Vector Autoregressive Model of US Natural Gas Markets*

Most Recent Version

Code

Valentin Winkler†

December 3, 2023

Abstract

This study uses a structural vector autoregressive (SVAR) model to examine the relationships between the intensity of drilling (i.e. investment) for natural gas, natural gas withdrawals, economic activity, and natural gas prices in the US. This yields the new result that the reaction of drilling to an unexpected natural gas price change depends on the source of the price change. Specifically, a price change due to economic activity shocks leads to a stronger drilling response than a price change due to different demand-side factors such as changing preferences or spillover effects from other energy markets. This can explain why natural gas drilling levels in the US were low after the Russian invasion of Ukraine despite the highest natural gas prices since 2008. In addition, I show that demand-side factors were more important than supply-side factors in explaining the 85 percent natural gas price drop from June 2008 to April 2012. This contradicts prevailing explanations focused on shale gas development and should dampen the expectations of policy makers seeking to rapidly expand shale gas production in order to obtain similar cheap energy as the US after 2008.

Keywords: Natural Gas, Drilling, Time Series, Structural VAR, Bayesian Inference

JEL Classification: C11, C32, Q41, Q43, Q48

*I am grateful to the IMK Düsseldorf for the opportunity to work on this project during a summer internship in 2022, and in particular to Sven Schreiber for his valuable suggestions and advice during this time. I would also like to thank Emanuel Gasteiger for help and guidance, Miriam Frauenlob for helpful remarks on the draft and the participants of the brown bag seminar of the TU Vienna Economics Research Group and the course Bayesian Econometrics II in spring 2023 at WU Vienna for their feedback and the opportunity to present my work.

†Mail: valentin.winkler@icloud.com

1 Introduction

The Russian invasion of Ukraine in spring 2022 has led to massive uncertainty about the security of natural gas supply in Europe. As a result, the determinants of fluctuations in natural gas supply and prices have become the focus of renewed attention. To gain additional empirical insights, this paper examines US natural gas markets using a structural vector autoregressive model. Understanding the US natural gas market is of global relevance: Since 2008, US-style gas on gas competition has largely replaced contracts linked to the oil price in many regions, among them the European Union (IGU, 2021; Mu, 2019). In addition, integration of local gas markets is advanced around the world, while this has been a reality in the USA for decades. One can thus look at the natural gas market in the US as a model towards which other markets are currently evolving.

US natural gas markets should also be studied, because in the last 15 years, their development has served as a blueprint for policy makers around the world. After decades of stagnation, natural gas production in the US started to rise rapidly between 2005 and 2007, which was mainly driven by a massive exploitation of unconventional natural gas reservoirs, commonly referred to as shale gas (Figure 1). After the financial crisis of 2008, the expansion of natural gas output was accompanied by a sharp decrease in prices, which fell by 85 percent between June 2008 and April 2012.[1] Since at that time global energy markets experienced surging prices (see Figure 2 and Mu, 2019), the governments of Argentina, Poland, and Australia, among others, tried to work on their own shale gas boom (Wang and Krupnick, 2015). Therefore, examining the causes of the post-2008 decline in natural gas prices in the US is of great importance. Misjudging the consequences of the US shale gas boom can lead to exaggerated expectations about the potential benefits of shale gas development. Such a faulty assessment carries the risk of accepting too great a financial and environmental cost when developing shale gas. This paper shows that demand-side factors contributed more to the 85 percent natural gas price drop between June 2008 and April 2012 than the shale gas boom. This suggests that policy makers should not expect as sharp a price drop as the US has experienced after 2008, even if they were as successful in expanding shale gas production.

One novelty of this paper is that in addition to economic activity, gas production, and the gas

[1] In June 2008 one MMBtu of natural gas (about 0.29 MWh) cost 12.7 USD at the Henry Hub, in April 2012 this price was down to 1.95 USD. Source: FRED (2022) 'Henry Hub Natural Gas Spot Price, Not Seasonally Adjusted (MHHNGSP)' (monthly): `https://fred.stlouisfed.org/series/MHHNGSP`.

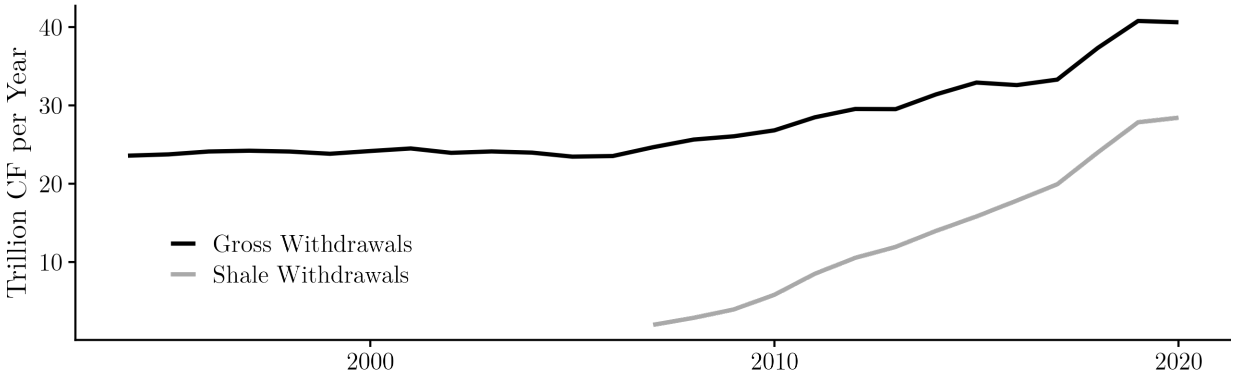

Figure 1: Natural gas withdrawals in the United States and the contribution of shale gas.
Source: Energy Information Administration (2022) 'Natural Gas Gross Withdrawals and Production' (annual): `https://www.eia.gov/dnav/ng/ng_prod_sum_dc_NUS_mmcf_a.htm`.

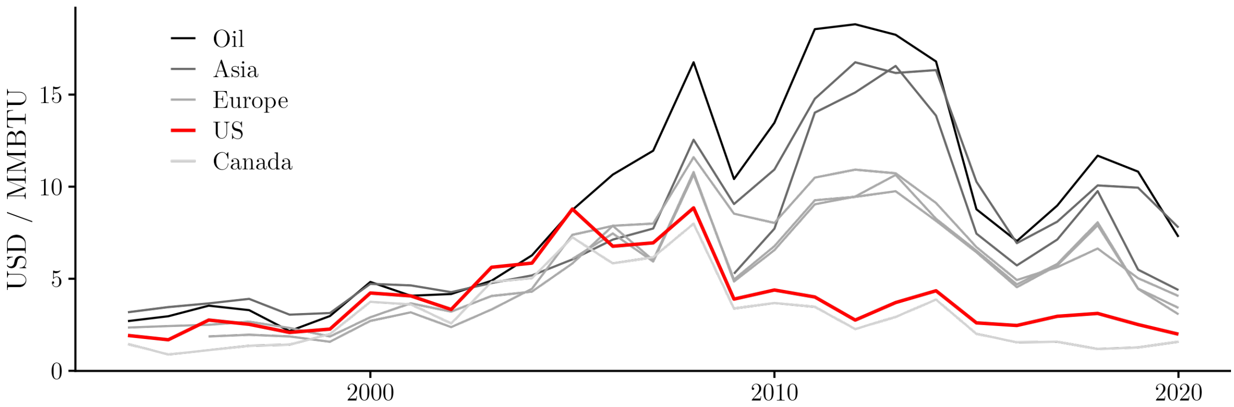

Figure 2: International natural gas and oil prices in comparison to US natural gas prices.
Source: Statistical Review of World Energy - BP via Our World in Data (2022) 'Natural gas prices' (annual): `https://ourworldindata.org/grapher/natural-gas-prices`.
Notes: Oil price is OECD crude oil price, Asian prices are 'Japan LNG (CIF)' and 'SE Asia LNG (JKM)', European prices are 'Dutch (TTF)', 'German Imports', 'UK (NBP)', US price is the 'Henry Hub' annual average and the Canadian price is the price in Alberta.

price I include natural gas drilling in my SVAR model. Since natural gas and oil production from existing wells depends primarily on geological characteristics rather than fuel prices, producers mainly respond to price fluctuations through the rate of drilling (see Anderson et al., 2018; Mason and Roberts, 2018, for oil and gas, respectively). Thus the rate of drilling is the most important supply-side decision variable of oil and gas companies. Nevertheless, there seems to be a lack of structural macro-econometric models trying to explain the determinants and effects of drilling. Existing papers on drilling mainly focus on the micro-level (Kellogg, 2011, 2014; Anderson et al., 2018) or conduct traditional time series analysis using reduced form equations, where general macroeconomic conditions are either ignored or treated as exogenous (Khalifa et al., 2017; Shakya et al., 2022). I find that the reaction of drilling to an unexpected natural gas price change strongly depends on the source of the price change. Price changes due to economic activity produce a larger reaction of drilling than price changes due to other demand-side factors, such as spillovers from oil markets or changed preferences. This new result could serve as an explanation for why natural gas drilling in the US was low after the Russian invasion of Ukraine, even though prices were the highest they had been since the great recession.

The remainder of the paper is structured as follows: In Section 2, I outline the debate on the role of supply and demand in explaining oil and natural gas price fluctuations, focusing on the time-series literature, and situate my work within it. Section 3 sets up the structural vector autoregressive model and explains how identification and inference are conducted. In Section 4, the main results are presented and discussed, Section 5 contains several robustness checks of my key results and Section 6 concludes.

2 Determinants of Oil and Natural Gas Price Fluctuations

The methods for analyzing natural gas markets using SVAR models build heavily on the work on oil markets. Since Kilian (2009), a consensus has developed that a large part of oil price fluctuations is due to variations in global oil demand. He arrives at his conclusions by setting up a structural vector autoregressive (SVAR) model that not only includes oil production and oil prices but also a measure of global economic activity. He finds demand that demand for oil stemming from changes in global economic activity was mainly responsible for rising prices in the 2000s, which explains why this oil price increase did not curb economic growth in the US. Kilian and Murphy (2012, 2014) further develop the basic model of Kilian (2009) by imposing inequality instead of exclusion restrictions. They confirm that oil prices are driven primarily by the demand side rather than the supply side. This conclusion has not gone unchallenged: Baumeister and Hamilton (2019) propose an innovative modeling approach that imposes a prior on the contemporaneous elasticities between endogenous variables and not on the instantaneous effects of the structural shocks. They find that supply-side shocks are more important drivers of oil prices than previous models have suggested. Kilian (2022) responds by arguing that this result depends on relaxing the constraint to the price elasticity of oil supply, for which there is no empirical justification. Recently, Braun (2023) has shown that the results of Baumeister and Hamilton (2019) that challenge Kilian and Murphy (2014) largely disappear if non-Gaussianity is employed for identification. Additional methodological debates in the oil market literature are summarized in Kilian and Zhou (2020).

In the past decade, SVARs have been increasingly employed to study natural gas markets. Arora and Lieskovsky (2014), Hou and Nguyen (2018) and Rubaszek and Uddin (2020) use some modification of the basic Kilian (2009) oil market model. They all report that demand-side factors are the main driver of natural gas prices, while supply-side factors play only a minor role. The two studies most closely related to this paper are Wiggins and Etienne (2017) and Rubaszek et al. (2021). The former use a identification strategy similar to Kilian and Murphy (2014) while the latter apply the oil market model of Baumeister and Hamilton (2019) to the natural gas market of the United States. Like this paper, both studies find that demand-side shocks played a major role in the decline of natural gas prices after 2008. Since they use competing modeling approaches, this speaks for the robustness of the result, especially since the Baumeister and Hamilton (2019) model allows for a larger contribution of supply-side factors to oil price fluctuations than the model of Kilian and Murphy (2014). However, neither study explicitly calculates the relative importance of demand-side shocks to the price drop in a given time window or performs inference on such a magnitude. To the best of my knowledge, this paper is the first to do so.

3 The Econometric Model

3.1 Structural Vector Autoregression

To model the US natural gas market, I propose a structural vector autoregressive (SVAR) model of the form

$$A_0 y_t = c + \sum_{j=1}^{p} A_j y_{t-j} + A_x x_t + \epsilon_t, \quad (\epsilon_t) \overset{iid}{\sim} N(0, I_4), \tag{1}$$

where y_t is an $n \times 1$ vector of endogenous variables and x_t is a $q \times 1$ vector of exogenous variables. The $n \times n$ matrix A_0 captures contemporaneous structural relationships between the endogenous variables, while the $n \times n$ matrices $A_1, ..., A_p$ and the $n \times q$ matrix A_x model the influence of past endogenous and current exogenous variables. Left-multiplying (1) by A_0^{-1} yields the reduced form

$$y_t = d + \sum_{j=1}^{p} B_j y_{t-j} + B_x x_t + e_t, \quad (e_t) \overset{iid}{\sim} N(0, \Sigma), \tag{2}$$

where $B := [d, B_1, ..., B_p, B_x] = A_0^{-1}[c, A_1, ..., A_p, A_x]$ and $\Sigma = A_0^{-1}(A_0^{-1})'$. To estimate the reduced form, I choose a Bayesian approach and propose a Gaussian-Inverse Wishart prior:

$$\Sigma \sim \mathcal{IW}_n(S_*, n_*), \quad \text{vec}(B)|\Sigma \sim N(\beta_*, V_* \otimes \Sigma), \tag{3}$$

I set the hyper-parameters $n_*, S_*, \beta_*, V_*^{-1}$ to zero, which yields an improper prior distribution. Since this is a natural conjugate prior, one can sample from the posterior distribution using an off-the-shelve random number generator after computing the posterior hyper-parameters. (see Kilian and Lütkepohl, 2018, p. 162-165 for details).

3.2 Data

To model the joint dynamics of macro-economic and gas-market specific conditions, I use four endogenous variables: A measure of active drilling rigs (r_t), gas production (q_t), industrial production (i_t) and the natural gas price (p_t). Therefore, the vector of endogenous variables looks as follows:

$$y_t' = \begin{bmatrix} y_{t1} & y_{t2} & y_{t3} & y_{t4} \end{bmatrix} = \begin{bmatrix} r_t & q_t & i_t & p_t \end{bmatrix}. \tag{4}$$

As a measure of drilling, r_t, I include the number of active rigs currently used for gas drilling in the United States as provided by the Baker Hughes Rig Count.[2] Since rigs are used to drill new wells and to deepen or sidetrack existing ones, their use serves as a broad measure of investment in natural gas development. Furthermore, since drilling is expensive and the economic viability of new production capacity is highly dependent on future prices (Mu, 2019), the rig count is a barometer of industry expectations. The most important reason to model drilling is recent research showing that the price elasticity of oil and natural gas production from existing wells is small, because production there is mainly determined by geological characteristics (Anderson et al., 2018; Mason and Roberts, 2018). Therefore, oil and gas producers mainly react to price changes via the drilling rate. This makes drilling a key variable for understanding natural gas markets.

The choice of the remaining endogenous variables largely follows the literature. Like Arora and Lieskovsky (2014) and Wiggins and Etienne (2017), I use marketed US natural gas with-

[2]Baker Hughes Rig Count via Energy Information Administration (2022) 'Crude Oil and Natural Gas Drilling Activity' (monthly): `https://www.eia.gov/dnav/ng/ng_enr_drill_s1_m.htm`.

drawals[3] as a measure of gas production, q_t, and real US industrial production[4] as i_t. While in oil market models it is common to include a *global* measure of economic activity, the US natural gas market can be considered as local.[5] Finally, as the gas price, p_t, the Henry Hub price deflated by the US consumer price index[6] is used. The monthly Henry Hub price is provided by the Wall Street Journal for 1993M11-2014M02.[7] From 1997M01 on a monthly Henry Hub series is made available by the EIA.[8] Like Arora and Lieskovsky (2014) I first use the Wall Street Journal series, but I switch to the EIA series when the former is discontinued.

Now I present the exogenous variables x_t. To account for natural gas usage in the residential sector due to temperature fluctuations, I follow Brown and Yücel (2008) as well as Nick and Thoenes (2014) and include measures of temperature. Heating or cooling degree days, as provided by the EIA[9], measure how cold or warm a certain location is. To assess national energy demand, local measures are population-weighted. I add dummy variables for each month to capture seasonal effects and to exclude two extraordinary events, the hurricanes Katrina in 2005M09 and Gustav in 2008M09. Katrina greatly reduced natural gas output, especially in the Gulf of Mexico, in an already tight market and led to a spike in prices (see DOE, 2006). Three years later, Gustav also reduced natural gas production but was not followed by a price hike since the Great Recession had reduced energy demand (see CRS, 2009). These hurricanes led to extraordinary short-term reductions of gas production, which violates the assumption of symmetric shocks. I also use a broken trend dummy of the form $\begin{bmatrix} 0 & ... & 0 & 1 & 2 & 3 & ... \end{bmatrix}$ to account for a constant rise in gas production from the mid 2000s onwards. As is described by Kellogg (2011), Anderson et al. (2018), Wang and Krupnick (2015) and Mu (2019), among many others, from the early 2000s on innovations in hydraulic fracturing ('fracking') and horizontal drilling led to higher cost effectiveness and production levels in the oil and gas industry. The start of this broken trend, 2005M05, is determined by applying the Bai and Perron (1998) procedure to

[3]Energy Information Administration (2022): 'US Natural Gas Marketed Production' (monthly): `https://www.eia.gov/dnav/ng/hist/n9050us2M.htm`

[4]FRED (2022) 'IPB50001N' (monthly): `https://fred.stlouisfed.org/series/IPB50001N`.

[5]Li et al. (2014) show that between 1997 and 2011 there is no evidence for convergence between North American and European or Asian natural gas prices. Especially after 2008 the lack of or fully utilised capacity for liquefied natural gas exports served as a physical barrier, that prevented North American gas prices from converging to the much higher world market level.

[6]FRED (2022) 'USACPIALLMINMEI' (monthly): `https://fred.stlouisfed.org/series/USACPIALLMINMEI`.

[7]Wall Street Journal via FRED (2016) 'GASPRICE' (monthly): `https://fred.stlouisfed.org/series/GASPRICE`.

[8]Energy Information Administration via FRED (2022) 'MHHNGSP' (monthly): `https://fred.stlouisfed.org/series/MHHNGSP`.

[9]Energy Information Administration (2022) 'Heating degree-days by census division' (monthly); 'Cooling degree-days by census division' (monthly): `https://www.eia.gov/totalenergy/data/monthly/index.php`

the output series q_t. Of course, the shale gas boom was not exogenous in reality. Innovations in hydraulic fracturing have been driven forward and made viable by various episodes of high energy prices, starting in the 1970s (Wang and Krupnick, 2015). Since the SVAR is not able to handle these decade-long lags, the broken trend is an auxiliary construction. As is shown in Section 5, the main results do not change when the broken trend is not included.

I use six lags of endogenous variables in my model, since according to Kilian and Zhou (2020) long lags are needed to capture the relationship between economic activity and oil market variables. Additionally, Kellogg (2014) and Khalifa et al. (2017) report that drilling takes multiple months to react to price changes. The endogenous variables are included in log-levels and the exogenous temperature series have the mean of the last five observations that were in the same month subtracted from itself to remove any possible trend as well as their seasonal pattern. Lastly, the SVAR model is estimated using monthly data starting in 1993M11 through 2020M01. I do not use data after the latter date because the Covid pandemic and the Russian invasion of Ukraine were such exceptional events that it is questionable whether the linear SVAR model is appropriate for this period. This may raise legitimate doubts about the external validity of the results of this study for the future, which depends on whether these extraordinary events fundamentally changed the functioning of energy markets in the long run. It is probably too early to tell, but caution is definitely warranted.

3.3 Identifying Assumptions

After estimating the reduced form (2), the structural form (1) is still to be identified. For a given reduced form model $[B, \Sigma]$ any set of structural parameters that satisfies

$$A_0^{-1} = CQ, \tag{5}$$

$$\begin{bmatrix} c & A_1 & \dots & A_p & A_x \end{bmatrix} = A_0 \begin{bmatrix} d & B_1 & \dots & B_p & B_x \end{bmatrix}, \tag{6}$$

is a corresponding structural model, where $C = \text{chol}(\Sigma)$ and $Q \in \mathcal{O}(n) := \{Q \in \mathbb{R}^{n \times n} | QQ' = Q'Q = I_n\}$ is an arbitrary orthonormal matrix. For identification, I restrict the values of A_0^{-1} using a-priori knowledge. Table 1 summarizes the sign and exclusion restrictions used. First, I assume that the first of the four structural shocks that span the innovations in the reduced form model is a drilling shock. It is the only shock that can affect the number of

	Drilling Shock	Gas Supply Shock	Economic Activity Shock	Gas Demand Shock
Rig Count	*	0	0	0
Gas Production	*	$-$	$+$	$+$
Ind. Production	*	$-$	$+$	$-$
Gas Price	*	$+$	$+$	$+$

Table 1: Impact sign and exclusion restrictions for A_0^{-1}.

Notes: Additional elasticity restrictions are described in the text.

active rigs contemporaneously, since for contractual, legal and technical reasons the decision to drill takes about three months to result in actual drilling activities (Kellogg, 2014). With this assumption, the first column of A_0^{-1} is point-identified. The second structural shock, a gas supply shock, decreases gas production unexpectedly, which increases the gas price and therefore decreases industrial production. The third shock, an economic activity shock, raises industrial production, which pushes the gas price up and thus triggers a rise in natural gas production. Lastly, a demand shock specific to the gas market raises gas prices and thus gas production while decreasing industrial production. A gas demand shock can be thought of as a shift in preferences, for example representing changed heating and cooling behavior or a transformation of energy production due to environmental concerns. Another possibility are spillover effects: Brown and Yücel (2008) and Nick and Thoenes (2014) report that crude oil prices are important drivers of US and German natural gas prices. In recent years, the decoupling of oil and US natural gas prices after the shale gas boom might have mitigated the influence of oil price shocks on the US gas price.

Some structural models that satisfy the impact sign restrictions may imply highly implausible elasticities between endogenous variables. Therefore, I use microeconometric evidence by Mason and Roberts (2018), who study natural gas wells in Wyoming. They estimate a price elasticity of natural gas production of 0.0262, which is almost exactly the value that Kilian and Murphy (2014) use for the oil market. Splitting the sample in four quartiles according to peak production rates gives a price elasticity of 0.0646 for the fourth quartile, which is the largest such value. To be prudent, I use this value as an upper bound for the impact price elasticity of natural gas supply. Letting a_{ij} denote the elements of A_0^{-1}, I discard all model draws, for which a_{23}/a_{43} or a_{24}/a_{44} are above this threshold. Kilian and Murphy (2012) also restrict the impact response of economic activity to a oil market specific demand shock. The numerical value for this restriction is the hardest to motivate empirically, so they choose an arbitrary value close to zero and conduct sensitivity tests for that threshold. I restrict the immediate impact of a gas demand shock on industrial production, a_{34}, to the interval $(-0.004, 0)$, where 0.004 is half the standard deviation of the reduced form error of industrial production. In addition, Hamilton (2013) provides the theoretically motivated approximation that the short-term energy price elasticity of GDP should equal to the energy bill as a fraction of GDP times the price-elasticity of energy demand. A conservative estimate of this quantity is about a third of the lower bound I use for a_{34}.[10]

3.4 Identification Procedure

When using sign or elasticity restrictions to identify a model it is common to proceed as follows (Kilian and Lütkepohl, 2018, 421-490):

1. Propose also a prior for Q on $\mathcal{O}(n)$, usually a uniform prior is used.
2. Sample from the prior distribution of Σ, B and (possibly multiple times per reduced form draw) Q. Drawing from a uniform distribution on $\mathcal{O}(n)$ can be done by drawing $n \times n$ matrices with independent standard normal entries, computing the QR decomposition and retaining the matrix Q.
3. Check if $\text{chol}(\Sigma)Q$ satisfies all the imposed restrictions. If yes, save the structural model with $A_0^{-1} = \text{chol}(\Sigma)Q$ and $\begin{bmatrix} c & A_1 & \dots & A_p & A_x \end{bmatrix} = A_0 B$.

This approach works, because when using sign restrictions the set of all structural parameters satisfying the sign restrictions has always positive Lebesgue measure in the set of all structural parameters in the non-degenerate case (Arias et al., 2018). Thus, one will always have a positive probability of drawing an admissible model. The probability of drawing a model that satisfies a zero restriction, however, is zero. This is why Arias et al. (2018) develop an algorithm to draw structural models that satisfy just the *zero* restrictions, after which all the models that do not satisfy the *sign* restrictions can be deleted. For my model, there is no need to apply this algorithm. The structural model satisfies the zero restrictions of Table 1 if and only if

$$Q = \begin{bmatrix} 1 & 0_{1\times3} \\ 0_{3\times1} & Q^* \end{bmatrix}, \tag{7}$$

[10] In 2008, the real US natural natural gas bill was the highest in the sample (Source: EIA, Today in Energy, September 9, 2021) and amounted to below 1.2 percent of GDP. Rubaszek et al. (2021) estimate a short term price elasticity of gas demand of -0.42. Even using the extremely cautious value of -1 for this elasticity yields a lower bound of roughly -0.0014 for the reaction of log-output to an unexpected price increase of 0.114 log-points – one standard deviation of the reduced form error of the real gas price.

where $Q^* \in \mathcal{O}(3)$ is an arbitrary orthonormal matrix. Therefore, one can use sub-rotations (Mumtaz and Surico, 2009) by proposing a uniform prior for the smaller-dimensional rotation Q^*. Afterwards, instead of sampling Q directly, one can sample $Q^* \in \mathcal{O}(3)$, build Q as in (7) and retain Q if the structural model satisfies the sign restrictions – the zero restrictions will be satisfied automatically due to the sampling procedure. This approach is not only fast and easy to implement, it also has a nice geometric interpretation, which I discuss in the Appendix.

3.5 Inference on Impulse Response Functions

When using SVAR models, one often wants to conduct inference on the structural impulse response functions (IRFs). The IRF $\theta_{ij,h}$ is the derivative of the endogenous variable i with respect to the structural shock j lagged by h periods. If the joint behavior of multiple IRFs $\theta_{ij,h}$ is of interest, point-wise confidence intervals will usually be too narrow (see Lütkepohl et al., 2020, for solutions to this multiple inference problem). For set identified models, there is the additional problem of which point estimate to report for the impulse response functions. Inoue and Kilian (2013) suggest to report the modal IRF as the point estimate and a corresponding highest density region as confidence band, which is both optimal given a Dirac Delta loss function (Inoue and Kilian, 2013, 2018).[11] In contrast to pointwise medians and quantile bands, these statistics preserve the shape of the identified IRFs and provide sufficiently broad confidence bands that contain the intended fraction $1-\alpha$ of all IRFs in the posterior distribution. In more detail, Inoue and Kilian (2013, 2018) suggest the following procedure:

1. Draw M structural models $\{\begin{bmatrix} A_0 & A_1 & \dots & A_p & A_x \end{bmatrix}_i\}_{i=1}^M$ and compute the IRFs $\{\Theta_i\}_{i=1}^M$.
2. Compute the posterior density $f_i = f(\Theta_i)$ for every IRF.
3. Compute the $(1-\alpha)$-quantile $f^{1-\alpha}$ of all IRF posterior values f_i.
4. Report the modal model as point estimate and the set $\mathcal{S}_\alpha$ as confidence region:

$$\hat{\Theta} := \underset{\Theta_i : i=1,..,M}{\arg\max} f(\Theta_i), \tag{8}$$

$$\mathcal{S}_\alpha := \{\Theta_i : f_i \geq f^{1-\alpha}\}. \tag{9}$$

Since I am especially interested in the shape of the impulse response functions I choose this

[11] Recently, Inoue and Kilian (2022) have generalized this approach using other loss functions than the Dirac Delta.

approach. The posterior density of the IRFs in my model is different from the one reported in Inoue and Kilian (2018), however, since I do not sample Q directly but draw the smaller-dimensional Q^* and construct Q as in (7). The IRF posterior density for this case is derived in the Appendix.

4 Results and Discussion

4.1 Natural Gas Market Dynamics

Figure 3 reports the modal impulse response function and a 68% highest density region that is constructed as described above. First, I investigate the determinants of natural gas prices: According to the modal model, the drilling shock has no impact on the gas price, while gas supply, economic activity and gas demand shocks rise the natural gas price between 5 and 8 percent on impact. This effect is only significant for the economic activity shock after six months and for the gas demand until five months after the shock. In addition, gas price changes after gas supply and economic shocks tend to be persistent, while after a gas demand shock most of the price effect disappears after about half a year.

As a next step, I present the response of drilling to the structural shocks. A drilling shock raises the rig count significantly and does so in a hump-shaped way. Moreover, according to the modal model, any price increase is followed by a positive reaction of drilling. This result is not only consistent with optimizing behaviour of natural gas producers but also with previous studies showing that the rate of drilling is sensitive to price changes (Anderson et al., 2018; Mason and Roberts, 2018). The size of the drilling response to a price change, however, seems to vary with the source of the shock. While the gas specific demand shock triggers the strongest price increase on impact, drilling reacts only relatively weak. The economic activity shock seems to have the largest impact on drilling. Apparently, the magnitude of the response of drilling to a change in the gas price not only depends on the initial size of this change but also on its source, i.e. on the structural shock that is responsible for the price change in the first place. This makes sense from a business point of view. While economic activity shocks lead to a sustained price increase that can be exploited for long, a price increase due to gas demand shocks disappears quickly. This is relevant for oil and gas producers since drilling takes time and is an investment for years if not decades (Anderson et al., 2018; Mu, 2019). The following section will test the claim made here more formally.

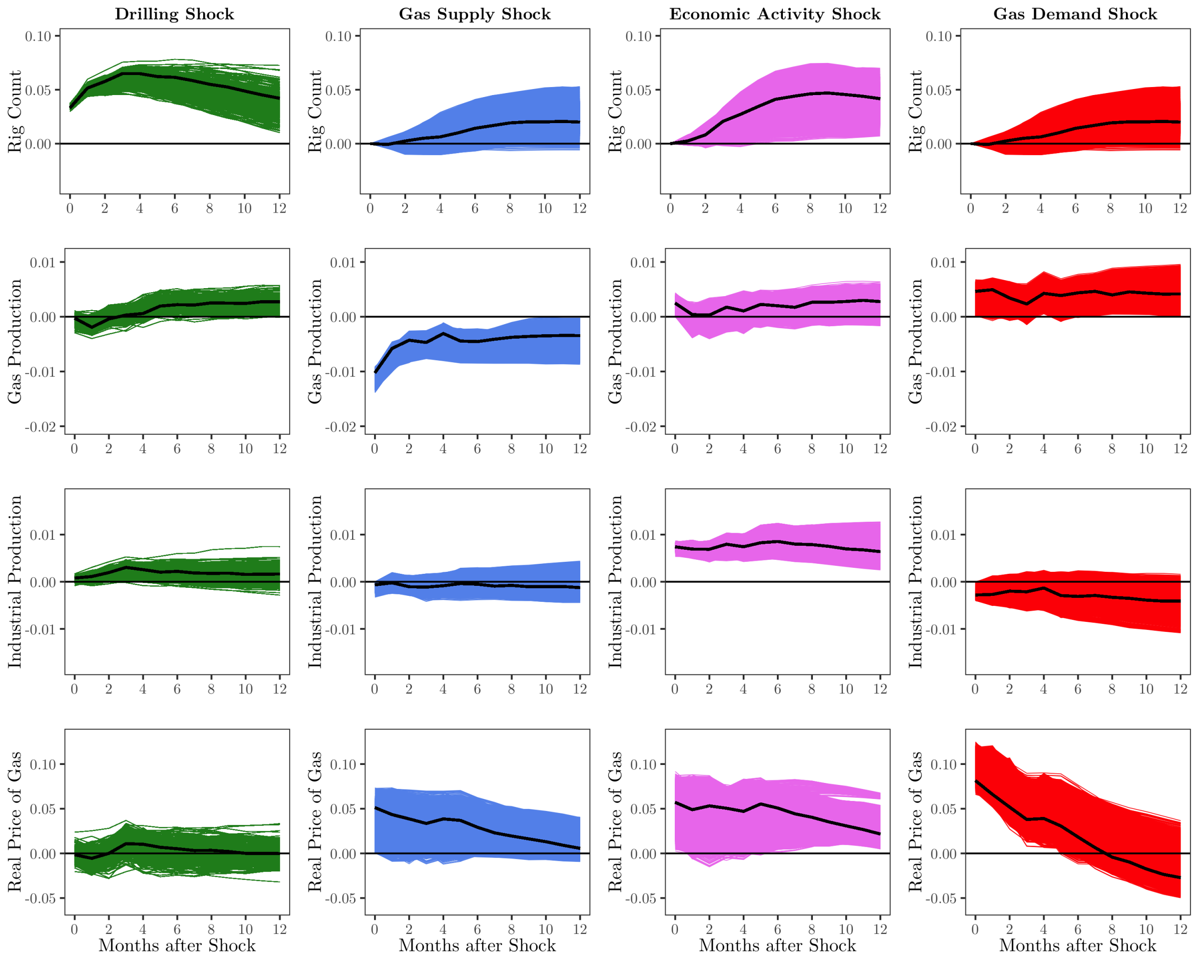

Figure 3: Structural impulse response functions.

Notes: Modal model and Bayesian 68% highest density region are constructed as defined in (8) and (9).

4.2 The Price Elasticity of Drilling

This section tests whether the drilling response to a change in the natural gas price depends on the shock that leads to the price change. Consider the following structural model:

$$r_t = \beta_h p_{t-h} + \eta_t, \tag{10}$$

where r_t is drilling, p_{t-h} is the natural gas price lagged by h periods, β_h is the dynamic price elasticity of drilling for horizon h and η_t is an error term. Suppose, the structural shock $\epsilon_{t-h,j}$ – which can be the gas supply shock, the economic activity shock or the gas specific demand shock – affects r_t only through p_{t-h}, then $\epsilon_{t-h,j}$ can be used as an instrument to estimate β_h:

$$\beta_h = \frac{\mathrm{Cov}(\epsilon_{t-h,j}, r_t)}{\mathrm{Cov}(\epsilon_{t-h,j}, p_{t-h})} = \frac{\theta_{1j,h}}{\theta_{4j,0}} =: \kappa_h^j, \tag{11}$$

where $\theta_{ij,h}$ is the impulse response of variable i to shock j after h periods. If the price elasticity of drilling does not depend on the source of the structural price shock, then the gas supply shock, the economic activity shock and the gas specific demand shock should yield the same κ_h^j.

For small horizons of two or three months the identifying assumption that $\epsilon_{t-h,j}$ only works through p_{t-h} might be plausible, since r_t is not able to react to $p_{t-h+1}, p_{t-h+2}...$ due to the sluggish nature of drilling.[12] This is clearly not the case for large h. In this case, one can make the weaker assumption that $\epsilon_{t,j}$ only affects the rig count through the price channel, regardless of the timing. Then κ_h^j is the response of r_t to changing $\{p_{t-h}, p_{t-h+1}, ..., p_t\}$ by $\{1, \theta_{4j,1}/\theta_{4j,0}, ..., \theta_{4j,h}/\theta_{4i,0}\}$. Therefore, a difference in κ_h^j for two different structural shocks does not need to be an indicator for β_h being different for the two shocks. Also differences in the dynamic price responses $\theta_{4j,1}/\theta_{4j,0}, \theta_{4j,2}/\theta_{4j,0}, ...$, i.e., the shape of of the IRFs, can be responsible for differences in κ_h^j. Even though for large h, κ_h^j does not identify β_h any more, it is still a meaningful measure. It tells how much more or less drilling one should expect h months after observing a one percent price change that is caused by the structural shock $\epsilon_{t,j}$.

Figure 4 plots the posterior densities of the differences $\kappa_h^{\text{econ. activity}} - \kappa_h^k$, where $k \in \{$gas supply, gas demand$\}$ for various horizons h. The value p denotes the fraction of models that imply a stronger drilling response after shock k than after the economic activity shock. The top panel shows that after one quarter, more than 85 percent of all models imply a stronger drilling response after an economic activity shock than after a gas supply shock. For a longer horizon, this difference vanishes. Compared to the gas demand shock, the economic activity shock produces a stronger drilling response with a high probability for every plotted horizon h. After a year, almost the whole posterior distribution of the IRFs implies a stronger drilling response after an economic activity shock than after a gas demand shock. The estimated magnitudes are also economically significant: The median and the 68 percent equal-tailed confidence intervals of the differences of the two drilling effects are 0.45 ([0.28, 0.73]), 0.58 ([0.38, 0.94]) and 0.65 ([0.44, 1.0]) after two, three and four quarters. Since for a six-month horizon the price effect of a gas demand shock is already gone, for large h part of the difference in κ_h^j might be due to the difference in the shape of the IRF. However, looking at the density plot for $h = 3$, one has reason to believe that also the elasticity β_h is smaller after a gas demand shock than after an economic activity shock. Oil and gas producers may already know that a demand-side shock that is not underpinned by strong economic performance will lead to price effects that are only short-lived.

[12] This is why Kellogg (2014) lagged oil price volatility by three months when regressing drilling onto it.

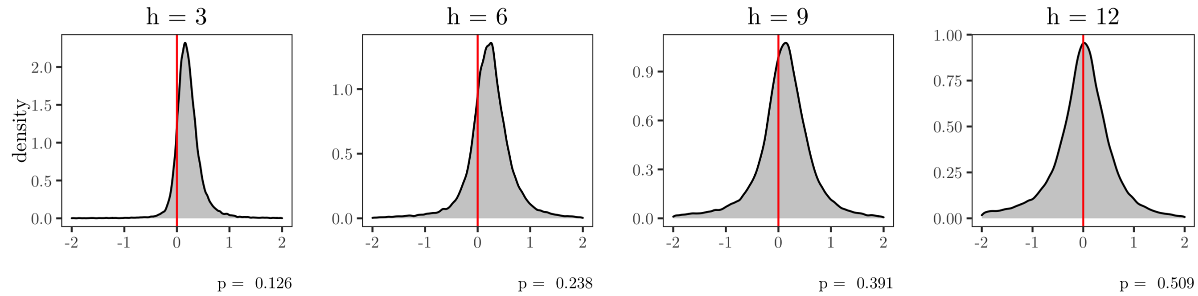

(a) $\kappa_h^{\text{econ. activity}} - \kappa_h^{\text{gas supply}}$

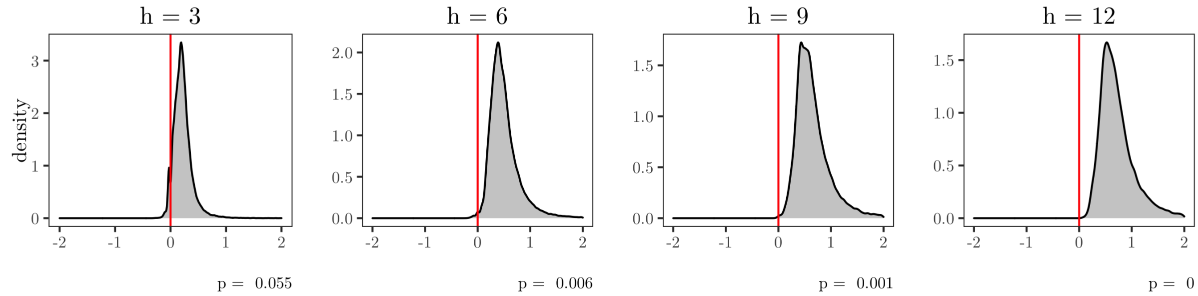

(b) $\kappa_h^{\text{econ. activity}} - \kappa_h^{\text{gas demand}}$

Figure 4: Posterior distributions of by how much *more* percentage points a one percent price change due to an economic activity shock raises drilling than the same price change after a gas supply (Panel a) or gas demand shock (Panel b).

Notes: This figure plots the posterior distribution of $\kappa_h^j - \kappa_h^k = \theta_{1j,h}/\theta_{4j,1} - \theta_{1k,h}/\theta_{4k,0}$ for two structural shocks for horizons of 1, 2, 3 and 4 quarters. The value p denotes the fraction of all models for which an economic activity shock produces a relatively lower reaction of drilling than the gas supply or gas demand shock.

This could explain why US natural gas drilling remained at low levels after Russia's invasion of Ukraine, despite the highest US natural gas prices since 2008.[13] Natural gas producers may have been uncertain whether prices would remain high for long, since they were not primarily driven by strong economic activity. In fact, by the winter of 2022 – about half a year after the war in Ukraine started – US natural gas prices had fallen to levels lower than before the war began.

4.3 Disentangling Historical Gas Price Fluctuations

To address what has historically been responsible for fluctuations in the price of US natural gas, I present a historical decomposition of the natural gas price conditional on the pre-sample. Let $\hat{p}_t^0$ be the natural gas price in period t that would have been experienced if no structural shocks had occurred after period zero. This is equal to $\mathbb{E}[p_t \mid \mathcal{I}_0, X]$, the expected price in period t

[13]The number of active natural gas rigs, according to the Baker Hughes rig count, never reached 170 in a month after the Russian invasion of Ukraine, while until December 2015 and between May 2017 and July 2019 the number of active rigs was never below 170 despite sometimes way lower natural gas prices. As a comparison: Between 2004 and 2008, the rig count was above 1000 for every single month.

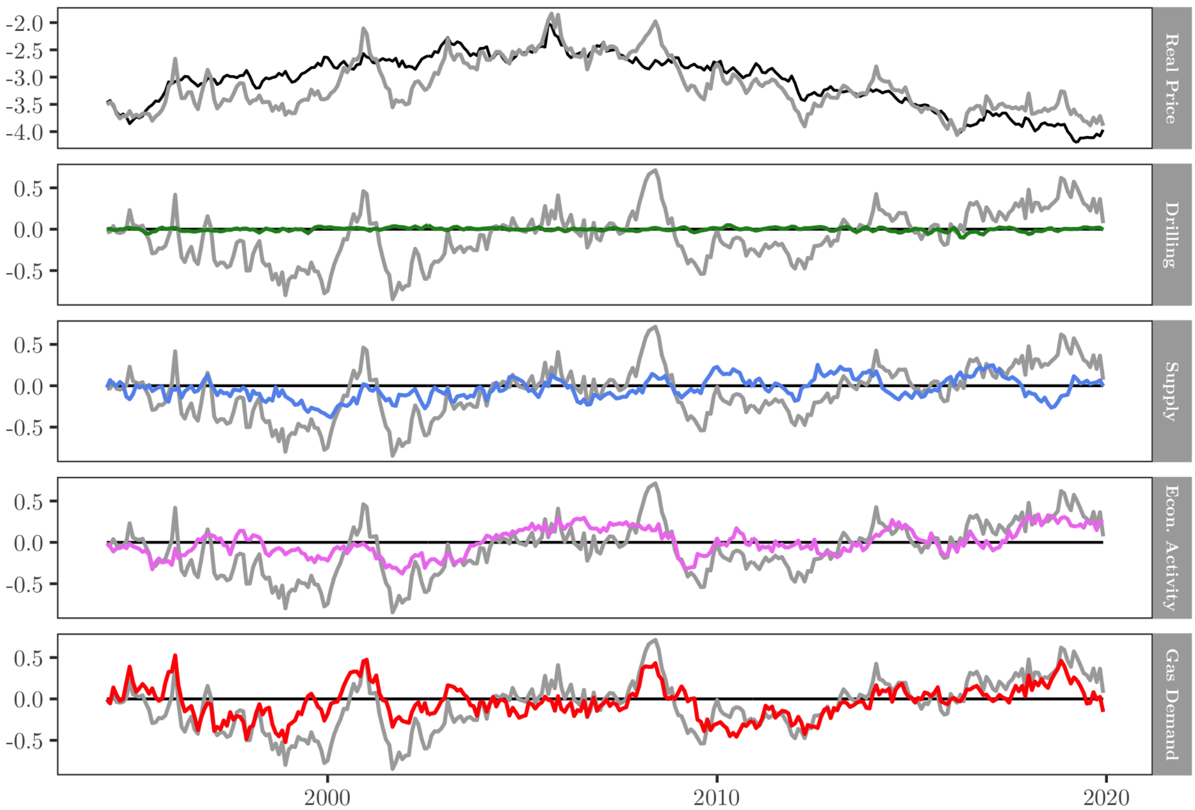

Figure 5: Historical decomposition of the natural gas price.

Notes: In the top panel, the comparison value $\hat{p}_t^0$ is plotted in black and the grey line is the true natural gas price p_t. The remaining panels present $(\hat{p}_t^i - \hat{p}_t^0)$ (color) as well as $(p_t - \hat{p}_t^0)$ (grey) for the four shocks.

conditional on information available at point zero as well as the exogenous variables. Similarly, $\hat{p}_t^i$, $i \in \{1, ..., n\}$ is the natural gas price if all shocks but i had been zero from $t = 1$ on and shock i had been as observed. The historical decomposition of all endogenous variables can be computed as

$$\hat{y}_t^i = d + \sum_{j=1}^{p} B_j \hat{y}_{t-j}^i + B_x x_t + A_0^{-1} \delta_i \epsilon_t, \tag{12}$$

where δ_i is a matrix of zeros with 1 as the i'th diagonal entry and $\begin{bmatrix} \hat{y}_{-p+1}^i & \dots & \hat{y}_0^i \end{bmatrix} := \begin{bmatrix} y_{-p+1} & \dots & y_0 \end{bmatrix}$. The resulting values have the property that

$$p_t - \hat{p}_t^0 = \sum_{i=1}^{n} \hat{p}_t^i - \hat{p}_t^0, \tag{13}$$

i.e., the deviation of the natural gas price from $\mathbb{E}[p_t \mid \mathcal{I}_0, X]$ can be decomposed into the contributions of the different structural shocks.

Figure 5 shows the historical decomposition for the real price of natural gas corresponding to the modal IRFs presented in Figure 3. The top panel plots the true gas price (in log-levels, grey line) together with the comparison value $\hat{p}_t^0$ (black), which rises until 2005 and declines afterwards. This can be attributed to the shale gas boom. The lower four panels plot the difference between the gas price and the comparison value (grey) together with the difference $\hat{p}_t^i - \hat{p}_t^0$ for the shock i (colored lines). If the latter value is positive for a given month, it means that the shock i pushed prices up at that time. The results largely match the economic calendar: Before 2000, natural gas prices were unusually low, which can be explained by extremely cheap oil after the Asian financial crisis.[14] In 2000 and 2001, natural gas prices spiked because of rising gas demand. During the California energy crisis, artificial tightening of electric energy supply and market manipulation led to a surge in demand for natural gas (see Wilson, 2002, for details on this event). Shortly afterwards prices fell, most likely due to the economic crisis in the aftermath of the Dotcom bubble and falling oil prices. Shortly before the great recession, natural gas prices went up sharply. Explanations for this are rising demand from the power generation and the residential sector (CRS, 2009) as well as record high oil prices. After this peak, the natural gas price was in free fall from 2008 to 2012. Note that it are demand-side factors and not supply changes due to the shale boom that seem to be mainly responsible for this price drop. This is not self-evident, since economists and market analysts have often attributed the drop of the natural gas price around the financial crisis to the shale boom (Wiggins and Etienne, 2017). Hausman and Kellogg (2015), for example, estimate that demand-side factors are responsible for less than 20 percent of the fall in natural gas prices between 2007 and 2013, while the shale gas revolution is argued to be responsible for the remainder. The question of what really caused the rapid decline in US energy prices after 2008 is highly relevant, as the US experience has served and continues to serve as a blueprint for many countries to develop shale gas resources themselves. It is therefore worth taking a closer look at this period.

4.4 What Drove Prices Down After 2008?

The price change between periods t and $t + h$ can be decomposed as follows:

[14] In November 1998, the nominal price for one Barrel of WTI was the lowest since 1986. Source: FRED (2022) 'DCOILWTICO' (monthly): `https://fred.stlouisfed.org/series/DCOILWTICO`.

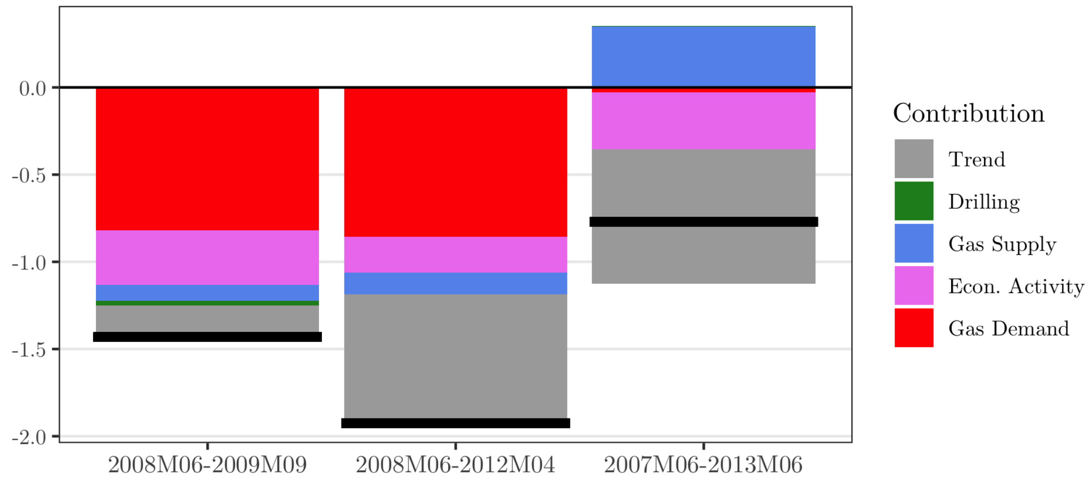

Figure 6: Contributions of trend and different shocks to natural gas price collapse around 2008. *Notes:* Solid lines mark changes in log real natural gas prices in two time windows. Colored bars represent contributions of fitted trend and different structural shocks to this price change that were computed using (14).

$$\begin{aligned} p_{t+h} - p_t &= (p_{t+h} - \hat{p}^0_{t+h}) + (\hat{p}^0_{t+h} - \hat{p}^0_t) + (\hat{p}^0_t - p_t) \\ &= \underbrace{(\hat{p}^0_{t+h} - \hat{p}^0_t)}_{C_0^{t,h}} + \sum_{i=1}^{n} \underbrace{\left[(\hat{p}^i_{t+h} - \hat{p}^0_{t+h}) + (\hat{p}^0_t - \hat{p}^i_t)\right]}_{C_i^{t,h}} . \end{aligned} \tag{14}$$

The $C_i^{t,h}$'s are the contributions of the n different shocks and $C_0^{t,h}$ is the contribution of the deterministic component. $C_0^{t,h}$ is assumed to capture large parts of the effects of the shale gas boom. Figure 6 plots the historical contributions to the gas price drop for three time-windows using the model of the modal IRF. After its peak in June 2008, the natural gas price reached a local minimum in September 2009. My model attributes more than three quarters of this fall to gas demand and economic activity shocks. Between June 2008 and April 2012 the gas price fell by a dramatic 85 percent. Here, too, the effect of demand-side shocks is estimated to be bigger than that of the supply-side factors. I also look at the time window June 2007 to June 2013 to establish some comparability with the results of Hausman and Kellogg (2015), even though they used annual data and therefore I do not estimate exactly the same quantity. Still, my model attributes more than 40 percent of the fall of the gas price to demand-side shocks, which is more than double the estimate of Hausman and Kellogg (2015).

To determine the uncertainty in the share of the gas price decline that is due to demand-side factors, one can directly calculate the posterior distribution of the following estimate:

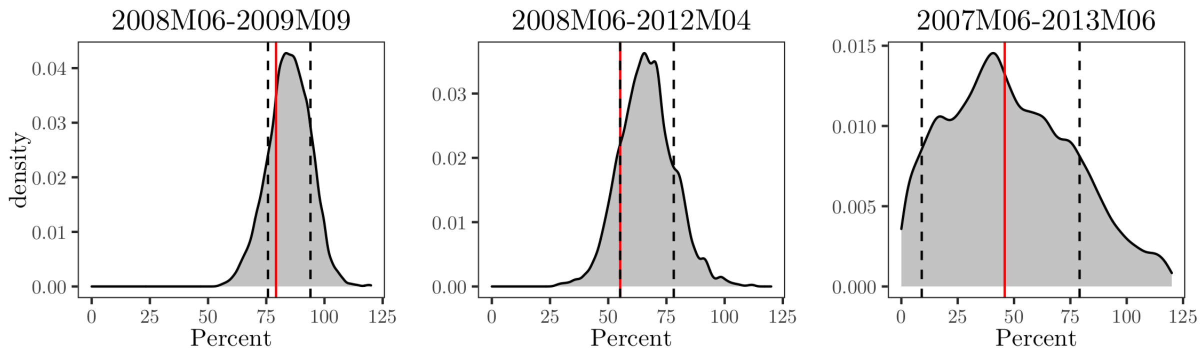

Figure 7: Posterior distribution of the fraction of the natural gas price drop that can be attributed to demand-side shocks (econ. activity and gas demand shocks) in three time intervals. *Notes:* Red line represents fraction that corresponds to the modal IRF, dotted lines are endpoints of the 68% equal-tailed confidence intervals. Plotted are distributions of the random variable defined in (15).

$$\frac{C^{t,h}_{\text{econ. activity}} + C^{t,h}_{\text{gas demand}}}{p_{t+h} - p_t} \times 100. \tag{15}$$

Figure 7 plots the posterior distribution of this variable for the time windows examined above. The graph also shows the value corresponding to the model in Figure 6 (red, solid) and a 68% equal-tailed confidence interval (black, dashed). The confidence interval is above 75 percent for the time window from June 2008 to September 2009 and still above 50 percent for the longer time window until April 2012. Thus, one can conclude that for the rapid price decline after 2008 demand-side factors were more important than the shale gas boom. For the six-year window June 2007 until June 2013, however, the estimate is so imprecise that it is not possible to reject any meaningful hypothesis about the role of supply and demand-side shocks in this period. In particular, the estimate of Hausman and Kellogg (2015), which also has a high variance, is covered by my confidence interval.

5 Robustness Checks

Key results in SVAR models often rely heavily on certain prior assumptions. For example, restrictions on the price elasticity of oil supply affect the importance of demand-side factors in explaining oil price fluctuations (Baumeister and Hamilton, 2019; Kilian, 2022; Braun, 2023). While it is the responsibility of the researcher to employ available prior information in order to not let economically implausible models dominate the posterior distribution, it is important to know how sensitive the results are to certain prior assumptions. Therefore I conduct the following robustness checks:

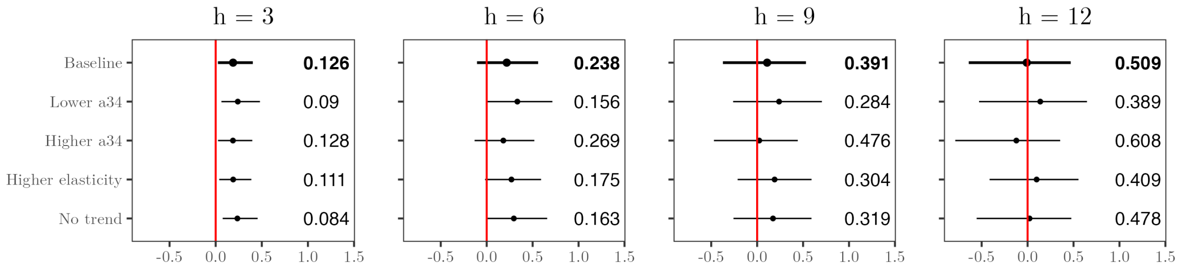

(a) $\kappa_h^{\text{econ. activity}} - \kappa_h^{\text{gas supply}}$

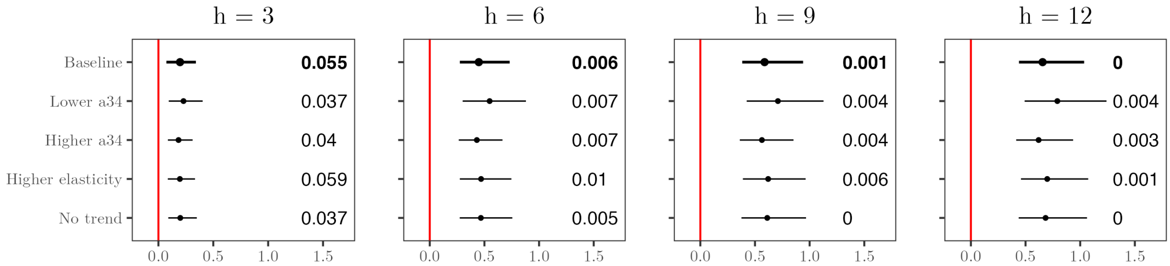

(b) $\kappa_h^{\text{econ. activity}} - \kappa_h^{\text{gas demand}}$

Figure 8: Robustness check: Differences of the drilling response to unexpected natural gas price changes by shock.

Notes: This figure plots the median as well as the equal-tailed 68 percent confidence interval for the posterior distribution of $\kappa_h^j - \kappa_h^k = \theta_{1j,h}/\theta_{4j,1} - \theta_{1k,h}/\theta_{4k,0}$ for the baseline model and various specifications. A positive value for this variable implies that drilling reacts stronger to price changes due to shock j than to price changes due to shock k. The numbers in the panels denote the fraction of all models where $\kappa_h^j \leq \kappa_h^k$.

- *Lower a34 / Higher a34.* The maximum impact of a gas specific demand shock on industrial production in the first month is neither strongly rooted in theory nor in empirics. Instead of -0.004, which is half the standard deviation of the reduced form error of industrial production times minus one, I use -0.0027 and -0.0053 as lower bounds, which are one-third and two-thirds of this standard deviation times minus one, respectively.

- *Higher elasticity.* My upper bound for the impact price elasticity of natural gas supply is already rather conservative. I chose the point estimate for the most productive quarter of all active rigs, as reported by Mason and Roberts (2018) (see Section 3.3). I re-run my analysis using 0.085 as an upper bound, which is two standard errors above the point estimate 0.065.

- *No trend.* I included a broken trend in the SVAR model to account for the shale gas boom. To check the robustness of my results to this modeling choice, I re-estimate the model without such a trend component.

Figure 8 plots the median as well as the equal-tailed 68 percent confidence band for the

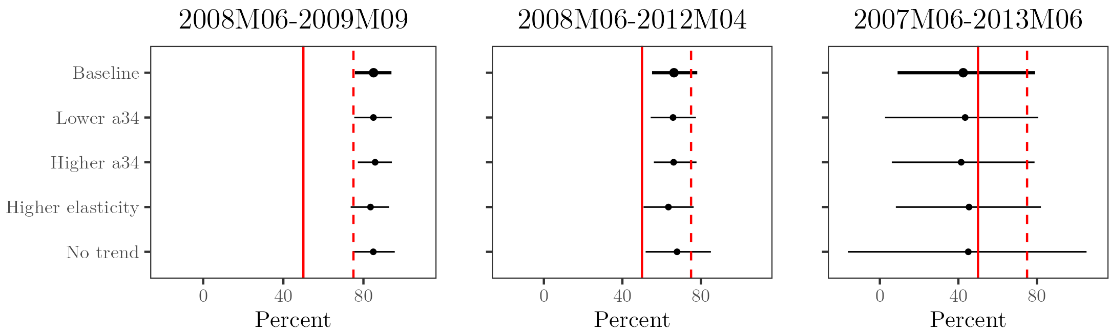

Figure 9: Robustness check: Fraction of the natural gas price drop that can be attributed to demand-side shocks (economic activity and gas demand shocks).
Notes: Plotted are the median as well as the 68 percent equal-tailed confidence band of the distribution of the random variable defined in (15) for the baseline model and various specifications. The solid and dashed red lines mark 50 and 75 percent, respectively.

posterior distributions of Figure 4. Also depicted are the fractions of all models for which the response of drilling to a price change is smaller after an economic activity shock than after a gas supply or gas specific demand shock, respectively. For every specification, price changes due to economic activity shocks lead to a stronger reaction of drilling than price changes due to other demand-side influences, especially for large horizons. The second result is also remarkably robust: Figure 9 shows that for all specifications the model attributes the majority of the natural gas price collapse after June 2008 to demand-side factors. The only visible difference occurs for the time window 2007M06-2013M06, where the confidence interval for the specification without trend is way broader than in the baseline model. This only confirms the conclusion that the demand-side contribution cannot be estimated precisely for this time period. All in all, my two main results are very robust with respect to the specific elasticity bounds and the modeling of a broken trend.

6 Conclusion

To study natural gas market dynamics in the United States, I set up a structural vector autoregressive model that includes the number of active drilling rigs, natural gas production, industrial production and the real price of gas. To identify the structural form, I employ a set of exclusion and sign restrictions. For conducting inference, I adapt the procedure of Inoue and Kilian (2013, 2018) that was originally designed for purely sign identified models.

As a new contribution, I find that the drilling response to unexpected natural gas price changes depends on the source leading to the price change. A price change due to an economic activity shock leads to a much stronger response in drilling than a price change due to different demand-side factors such as changing preferences or spillover effects from oil markets. One explanation is that economic activity shocks lead to persistent price changes, while the effects of the latter shock on the price of natural gas disappear quickly, so higher prices cannot be exploited for long. This may explain the low level of natural gas drilling in the US after Russia's invasion of Ukraine, despite the highest US natural gas prices since 2008. Natural gas producers had every reason to be skeptical about the duration of the price increases, as it was not primarily driven by strong economic activity. Since previous studies such as Anderson et al. (2018) and Mason and Roberts (2018) have found that oil and gas producers increase their supply primarily through drilling, this finding is highly relevant for policy makers seeking to expand domestic energy production.

Expanding natural gas production is usually not an end in itself. Governments typically hope that greater supply will lead to cheaper energy for national businesses and the electorate. It is therefore worthwhile to disentangle the reasons for the US natural gas price collapse around the financial crisis. Hausman and Kellogg (2015) attribute this fall to the shale gas revolution and estimate that demand-side factors are responsible for less than 20 percent of the total price drop between 2007 and 2013. Although the variance of my estimate for the period 2007 to 2013 is too high to reject the Hausman and Kellogg (2015) estimate, my model suggests that demand-side shocks were extremely important for explaining the drop in natural gas prices immediately after the financial crisis. Between June 2008 and April 2012, natural gas prices fell by an impressive 85 percent. I show that demand-side factors were more important than the shale gas boom in explaining the price decline during this time window. This should dampen the hopes of governments working on their own shale gas booms. As follows from Wang and Krupnick (2015) and Mu (2019), most countries lack one or many of the peculiarities that allowed for the massive boom in shale gas extraction in the United States.[15] However, even with a comparatively rapid expansion of natural gas production, no one should expect a price decline similar to that seen in the US after 2008.

[15] Examples for this are water availability, deep capital markets, a dynamic service-sector industry and the specific market structure of the oil and gas industry in the United States.

References

S. T. Anderson, R. Kellogg, and S. W. Salant. Hotelling under pressure. *Journal of Political Economy*, 126(3):984–1026, June 2018.

J. E. Arias, J. F. Rubio-Ramírez, and D. F. Waggoner. Inference based on structual vector autoregressions identified with sign and zero restrictions: Theory and applications. *Econometrica*, 86(2):685–720, March 2018.

V. Arora and J. Lieskovsky. Natural gas and u.s. economic activity. *The Energy Journal*, 35 (3):167–182, July 2014.

J. Bai and P. Perron. Estimating and testing linear models with multiple structural changes. *Econometrica*, 66(1):47–78, January 1998.

C. Baumeister and J. D. Hamilton. Structural interpretation of vector autoregressions with incomplete identification. *American Economic Review*, 109(5):1873–1910, May 2019.

R. Braun. The importance of supply and demand for oil prices: Evidence from non-gaussianity. *Quantitative Economics*, 14(1):1163–1198, 2023.

S. P. A. Brown and M. K. Yücel. What drives natural gas prices? *The Energy Journal*, 29(2): 45–60, 2008.

CRS. Natural gas markets: An overview of 2008. Congressional Research Service Report for Congress, 2009.

DOE. Impact of the 2005 hurricanes on the natural gas industry in the gulf of mexico region. United States of America Department of Energy Report, 2006.

J. D. Hamilton. *Handbook on Energy and Climate Change*, chapter Oil Prices, Exhaustible Resources, and Economic Growth, pages 29–63. Edward Elgar Publishing, 2013.

C. Hausman and R. Kellogg. Welfare and distributional implications of shale gas. *Brookings Papers on Economic Activity*, pages 71–125, 2015.

C. Hou and B. H. Nguyen. Understanding the us natural gas market: A markov switching var approach. *Energy Economics*, 75:42–53, 2018.

IGU. Wholesale gas price survey: A global review of price formation mechanisms. Technical report, International Gas Union, 2021.

A. Inoue and L. Kilian. Inference on impulse response functions in structural var models. *Journal of Econometrics*, 177(1):1–13, 2013.

A. Inoue and L. Kilian. Corrigendum to "inference on impulse response functions in structural var models". *Journal of Econometrics*, 209(1):139–143, March 2018.

A. Inoue and L. Kilian. Joint bayesian inference about impulse responses in var models. *Journal of Econometrics*, 231(2):457–476, December 2022.

R. Kellogg. Learning by drilling: Interfirm learning and relationship persistence in the texas oilpatch. *Quarterly Journal of Economics*, 126(4):1961–2004, November 2011.

R. Kellogg. The effect of uncertainty on investment: Evidence from texas oil drilling. *American Economic Review*, 104(6):1698–1734, June 2014.

A. Khalifa, M. Caporin, and S. Hammoudeh. The relationship between oil prices and rig counts: The importance of lags. *Energy Economics*, 63:213–226, 2017.

L. Kilian. Not all oil price shocks are alike: Disentangling demand and supply shocks in the crude oil market. *American Economic Review*, 99(3):1053–1069, June 2009.

L. Kilian. Facts and fiction in oil market modeling. *Energy Economics*, 110:105973, 2022.

L. Kilian and H. Lütkepohl. *Structural vector autoregressive analysis*. Themes in modern econometrics. Cambridge University Press, 2018.

L. Kilian and D. P. Murphy. Why agnostic sign restrictions are not enough: understanding the dynamics of oil market var models. *Journal of the European Economic Association*, 10(5): 1166–1188, October 2012.

L. Kilian and D. P. Murphy. The role of inventories and speculative trading in the global market for crude oil. *Journal of Applied Econometrics*, 29(3):454–478, April/May 2014.

L. Kilian and X. Zhou. The econometrics of oil market var models. *Federal Reserve Bank of Dallas Working Paper*, March 2020.

C. A. León, J.-C. Massé, and L.-P. Rivest. A statistical model for random rotations. *Journal of Multivatiate Analysis*, 97(2):412–430, 2006.

R. Li, R. Joyeux, and R. D. Ripple. International natural gas market integration. *The Energy Journal*, 35(4):159–179, October 2014.

H. Lütkepohl, A. Staszewska-Bystrova, and P. Winker. Constricting joint confidence bands for impulse response functions of var models - a review. *Econometrics and Statistics*, 13:69–83, 2020.

J. R. Magnus. *Linear structures.* Oxford University Press, 1988.

C. F. Mason and G. Roberts. Price elasticity of supply and productivity: An analysis of natural gas wells in wyoming. *The Energy Journal*, 39(1):79–100, 2018.

X. Mu. *The Economics of Oil and Gas.* Agenda Publishing, 2019.

H. Mumtaz and P. Surico. The transmission of international shocks: A factor-augmented var approach. *Journal of Money, Credit and Banking*, 41(1):71–100, February 2009.

S. Nick and S. Thoenes. What drives natural gas prices? a structural var approach. *Energy Economics*, 45(C):517–527, 2014.

M. Rubaszek and G. S. Uddin. The role of underground storage in the dynamics of the us natural gas market: A threshold model analysis. *Energy Economics*, 87, 2020.

M. Rubaszek, K. Szafranek, and G. S. Uddin. The dynamics and elasticities on the u.s. natural gas market. a bayesian structural var analysis. *Energy Economics*, 103, 2021.

J. F. Rubio-Ramírez, D. F. Waggoner, and T. Zha. Structural vector autoregressions: Theory of identification and algorithms for inference. *The Review of Economic Studies*, 77(2):665–696, April 2010.

S. Shakya, B. Li, and X. Etienne. Shale revolution, oil and gas prices, and drilling activities in the united states. *Energy Economics*, 108, 2022.

H. Uhlig. What are the effects of monetary policy on output? results from an agnostic identification procedure. *Journal of Monetary Economics*, 52:381–419, 2005.

Z. Wang and A. Krupnick. A retrospective review of shale gas development in the united states: What led to the boom? *Economics of Energy and Environmental Policy*, 4(1):5–17, 2015.

S. Wiggins and X. L. Etienne. Turbulent times: Uncovering the origins of us natural gas price fluctuations since deregulation. *Energy Economics*, 64:197–205, 2017.

J. F. Wilson. High natural gas prices in california, 2000-2001: Causes and lessons. *Journal of Industry, Competition and Trade*, 2(1-2):39–57, June 2002.

Appendix A. On Rotations and Sub-Rotations

This section presents proofs and additional intuition for statistical claims made in the paper. Most ideas are not new, I rather give them in a form that helped me understand in depth how the modeling approach of this project actually works. See Mumtaz and Surico (2009) for an example of sub-rotations similar to mine and Rubio-Ramírez et al. (2010) as well as Arias et al. (2018) for a more general treatment of identification in structural vector autoregressive models.

A.1 The Role of Rotations

For the sake of completeness, I proof a central and well known result for sign identified SVARs (see for example Uhlig, 2005, Proposition A.1).

Proposition 1 *Suppose $A, \Sigma \in \mathbb{R}^{n \times n}$ are of full rank, Σ is symmetric and positive definite. Then $AA' = \Sigma$ if and only if $A = CQ$, where $Q \in \mathcal{O}(n)$ is an arbitrary rotation matrix and $C = chol(\Sigma)$.*

Proof. Suppose $A = CQ$, then

$$AA' = CQQ'C' = CC' = \Sigma. \tag{16}$$

Now let A satisfy $AA' = \Sigma$ and calculate

$$A = C\overbrace{C^{-1}A}^{\tilde{Q}:=}, \tag{17}$$

where $\tilde{Q} \in \mathcal{O}(n)$ because

$$\begin{aligned}\tilde{Q}\tilde{Q}' &= C^{-1}AA'(C^{-1})' \\ &= C^{-1}\Sigma(C^{-1})' \\ &= C^{-1}CC'(C')^{-1} = I_n,\end{aligned}$$

and similarly $\tilde{Q}'\tilde{Q} = I_n$. ■

This property enables Arias et al. (2018) to use an alternative parametrization of the structural model (1), which they call the Orthogonal Reduced-Form Parametrization:

$$y_t = d + \sum_{j=1}^{p} B_j y_{t-j} + B_x x_t + \text{chol}(\Sigma) Q \epsilon_t, \quad (\epsilon_t) \overset{iid}{\sim} N(0, I_4), \tag{18}$$

which is convenient for sampling. When using this parametrization it is obvious that

$$e_t = CQ\epsilon_t \Leftrightarrow C^{-1}e_t = Q\epsilon_t, \tag{19}$$

where e_t is the reduced form error and $C^{-1}e_t$ is the 'structural' shock one would identify when using a recursive identification strategy. Thus one can always obtain a rotated version of the structural shocks. This is intuitive when interpreting mean-zero random variables with finite variance as vectors in a Hilbert space.[16] Identifying structural shocks amounts to finding *the* coordinate system (in terms of linear algebra *the* orthonormal basis) that spans the observed vectors $e_{t,i}$. Since there exist infinitely many such systems, the desired coordinate system cannot be found without additional information. It is clear, however, that every linear function that

[16] Here the length of a vector is its standard deviation and the inner product of two vectors is their covariance.

maps one coordinate system into another must preserve the length of and the angle between all vectors – in other words, it has to be a rotation. Therefore, it is geometrically intuitive that the identification of structural shocks can be broken down into two steps, orthonormalization and rotation, which amounts to multiplying the reduced form errors by C^{-1} and then Q.

A.2 Why Sub-Rotations Work

Consider a setting in which it is known that $A_0^{-1} \in \mathbb{R}^{n\times n}$ has the following form:

$$A_0^{-1} = \begin{bmatrix} A_{11} & 0_{n_1\times n_2} & \cdots & 0_{n_1\times n_k} \\ A_{21} & A_{22} & \cdots & 0_{n_2\times n_k} \\ \vdots & \vdots & \ddots & \vdots \\ A_{k1} & A_{k2} & \cdots & A_{kk} \end{bmatrix}, \tag{20}$$

where $A_{ij} \in \mathbb{R}^{n_i\times n_j}$ and $n = n_1 + ... + n_k$. In other words, A_0^{-1} is block lower-triangular. Unless $n_1 = ... = n_k = 1$, in which case one can just apply the Cholesky identification scheme, it is still not possible to exactly identify A_0^{-1}. However, the set of admissible models can be restricted, which is shown by the next Proposition:

Proposition 2 *Suppose $A, \Sigma \in \mathbb{R}^{n\times n}$ are of full rank. Σ is positive definite and symmetric. Furthermore, A is block lower triangular, i.e. there exist $n_1 + ... + n_k = n$ such that A consists of k^2 block matrices $A_{ij} \in \mathbb{R}^{n_i\times n_j}$ with $A_{ij} = 0_{n_i\times n_j}$ for $j > i$. Then $AA' = \Sigma$ if and only if $A = CQ$, where $C = chol(\Sigma)$ and $Q = diag(Q_1, ..., Q_k)$ is block-diagonal with $Q_i \in \mathcal{O}(n_i)$.*

Proof. Following Proposition 1 it is clear that A must have the form

$$A = CQ, \tag{21}$$

with $Q \in \mathcal{O}(n)$. Since C is lower triangular, C^{-1} is lower triangular and in particular block lower triangular as defined above. Therefore $Q = C^{-1}A$ is the product of two block lower triangular matrices. Using the same partition as for A, one can compute each of the k^2 blocks of Q as

$$Q_{ij} = (C^{-1}A)_{ij} = \sum_{s=1}^{k} (C^{-1})_{is} A_{sj}. \tag{22}$$

Now suppose $j > i$. Then for $s = 1, ..., j-1$ the matrix A_{sj} consists only of zeros and for $s = j, ..., k$ the same is true for matrix $(C^{-1})_{is}$. In this case, the right side of (22) is a sum of zero matrices and Q_{ij} consists of zeros only. Thus Q is also block lower triangular. As a next step, I prove that using the same partition, every orthonormal matrix Q that is block lower triangular is in fact block diagonal with orthonormal matrices as diagonal entries. For $k = 1$ this statement is trivial. Now suppose it holds for a certain k and take an arbitrary matrix $Q \in \mathcal{O}(n)$ with a partition corresponding to $n_1 + ... + n_{k+1} = n$ such that Q is block lower triangular. One can then partition this matrix into

$$Q = \begin{bmatrix} Q_{11} & 0_{n_1\times n_\bullet} \\ Q_{\bullet 1} & Q_{\bullet\bullet}, \end{bmatrix}, \tag{23}$$

where Q is of dimension $n_1 \times n_1$, $Q_{\bullet 1}$ is of dimension $n_\bullet \times n_1$ with $n_\bullet = n_2 + ... + n_{k+1}$ and $Q_{\bullet\bullet}$ is of dimension $n_\bullet \times n_\bullet$. Note that $Q_{\bullet\bullet}$ is block lower triangular with k^2 blocks. One can then use the fact that $Q \in \mathcal{O}(n)$:

$$QQ' = \begin{bmatrix} Q_{11} & 0_{n_1\times n_\bullet} \\ Q_{\bullet 1} & Q_{\bullet\bullet} \end{bmatrix} \begin{bmatrix} Q'_{11} & Q'_{\bullet 1} \\ 0_{n_\bullet\times n_1} & Q'_{\bullet\bullet} \end{bmatrix} = \begin{bmatrix} Q_{11}Q'_{11} & Q_{11}Q'_{\bullet 1} \\ Q_{\bullet 1}Q'_{11} & Q_{\bullet 1}Q'_{\bullet 1} + Q_{\bullet\bullet}Q'_{\bullet\bullet} \end{bmatrix} \stackrel{!}{=} \begin{bmatrix} I_{n_1} & 0_{n_1\times n_\bullet} \\ 0_{n_\bullet\times n_1} & I_{n_\bullet} \end{bmatrix}. \tag{24}$$

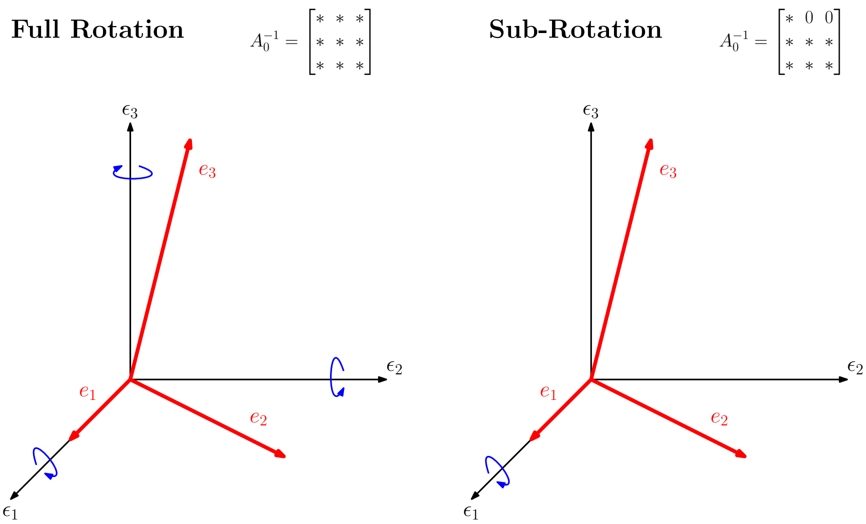

Figure 10: Difference between Rotations and Sub-Rotations.

Notes: The plotted coordinated system is the set of structural shocks obtained using the 'Cholesky-strategy'. Possible rotations of the coordinate system under the identification assumptions are drawn on the axes.

One can derive similar conditions from $Q'Q \overset{!}{=} I_n$. It follows immediately that $Q_{11} \in \mathcal{O}(n_1)$. Thus left-multiplying $Q_{11}Q'_{\bullet 1}$ by Q'_{11} yields $Q_{\bullet 1} = 0_{n_\bullet \times n_1}$ which implies $Q_{\bullet\bullet} \in \mathcal{O}(n_\bullet)$. Therefore $Q_{\bullet\bullet}$ is an orthonormal, block lower triangular matrix with k^2 blocks which, by induction assumption, is block diagonal with orthonormal matrices as diagonal entries. It follows that the statement holds also for $k+1$ and therefore for all $k \geq 1$, which finishes the proof. ■

It follows from Proposition 2 that for the model of this paper it must hold that $A_0^{-1} = \text{chol}(\Sigma)Q$ with Q being as given in (7). This result has a nice geometric interpretation. Let us re-write (19), using the special properties of Q in the case of A_0^{-1} being block lower-diagonal:

$$\begin{bmatrix} u_{t,m_1:n_1} \\ u_{t,m_2:n_2} \\ \vdots \\ u_{t,m_k:n} \end{bmatrix} := C^{-1}e_t = Q\epsilon_t = \begin{bmatrix} Q_1\epsilon_{t,m_1:n_1} \\ Q_2\epsilon_{t,m_2:n_2} \\ \vdots \\ Q_k\epsilon_{t,m_k:n} \end{bmatrix}, \tag{25}$$

where $m_s := n_1 + ... + (n_{s-1}+1)$, $m_1 := 1$ and $\epsilon'_{t,u:v} := [\epsilon_u \quad \epsilon_{u+1} \quad \cdots \quad \epsilon_v,]$ for $v > u$. Note that to obtain the true structural shocks ϵ_t one does not have to rotate $C^{-1}e_t$ in the whole n-dimensional space. Since $u_{t,m_j:n_j}$ only consists of $n_j \leq n$ of the structural shocks, sub-spaces of structural shocks are identified by the zero restrictions and Q is not allowed to map between these sub-spaces, which is represented by the zero-blocks off the diagonal of Q. Note that in the case of $n_i = 1$ for a block $i \leq k$ it follows from (25) that $\epsilon_{t,i}$ is a scaled version of $u_{t,i}$ and therefore this shock is point-identified up to sign, which is the case with the drilling shock in this paper's model. Figure 10 gives a geometric example of how sub-rotations narrow down the set of admissible rotations: Since the first axis of the coordinate system is identified through zero restrictions, rotations are not allowed to move it. This severely restricts the directions in which the system can be rotated. In summary, if one can plausibly impose block lower-triangularity on A_0^{-1}, sub-rotations allow to separate the space of all structural shocks into multiple smaller blocks of structural shocks, for which strategies such as sign or elasticity restrictions can be used to further narrow down the set of admissible rotations Q.

Appendix B. Derivation of the IRF Posterior Density

In the case of sign restrictions, Inoue and Kilian (2013, 2018) show that one can explicitly derive the posterior density of the structural impulse response functions Θ as

$$f(\Theta) = \left| \frac{\partial vec(\Theta)}{\partial [vec(B)' \; vech(C)' \; s']} \right|^{-1} \left| \frac{\partial vech(\Sigma)}{\partial vech(C)} \right| f(B|\Sigma) f(\Sigma) f(s), \tag{26}$$

where $S = I_n - 2(I_n + \tilde{Q})^{-1}$, $s = veck(S)$, $C = \text{chol}(\Sigma)$ and the operators vec, $vech$ and $veck$ stack the columns, lower triangular and sub-diagonal elements of a matrix, respectively. $\tilde{Q}$ is Q manipulated to satisfy $|\tilde{Q}| = 1$. For the remainder of the section, when I write Q, I will refer to $\tilde{Q}$. The matrix B is defined as $[B_1, ..., B_p]$. León et al. (2006) show that for a uniform distribution on $\{Q \in \mathcal{O}(n) || Q| = 1\}$ the variable s has the density function

$$f(s) = \left(\prod_{i=2}^{n} \frac{\Gamma(i/2)}{\pi^{i/2}} \right) \frac{2^{(n-1)(n-2)/2}}{|I_n + S|^{n-1}}. \tag{27}$$

In the case of my model identified using sub-rotations, I derive the posterior density of the IRFs as:

$$f(\Theta) = \overbrace{\left| \frac{\partial vec(\tilde{\Theta})}{\partial [vec(B)' \; vech(C)' \; (s^*)']} \right|^{-1}}^{I} \overbrace{\left| \frac{\partial vech(\Sigma)}{\partial vech(C)} \right| f(B|\Sigma) f(\Sigma) f(s^*)}^{II}. \tag{28}$$

where $s^* = veck(S^*)$ and $S^* = I_{n-1} - 2(I_{n-1} + Q^*)^{-1}$. The matrix Q^* is the one used to construct Q like in (7). For II, the formulas of Inoue and Kilian (2018) can be used. Only deriving I needs some tedious computations. Before that, however, I should introduce some notation: Let D_n be the $n^2 \times n(n+1)/2$ duplication matrix such that $\vec{(M)} = D_n \text{vech}(M)$ for any $n \times n$ symmetric matrix M. $\tilde{D}_{n-1}$ is the $(n-1)^2 \times (n-1)(n-2)/2$ matrix designed to satisfy $vec(S^*) = \tilde{D}_{n-1} s^*$. Similarly, L_n is $n(n+1)/2 \times n^2$ such that $vec(M) = L_n' vech(M)$ for any lower triangular matrix M. The $n \times 1$ vector e_i^n consists of zeros with only the i'th element being equal to one, c_{ii} is the i-th diagonal element of C. Lastly, the $n \times (n-1)$ matrix K is defined as $K' = [0_{(n-1)\times 1}, I_{n-1}.]$

Now I can proof the following Proposition:

Proposition 3 *Suppose the SVAR model 1 satisfies $A_0^{-1} = chol(\Sigma)Q$, with $Q = diag(1, Q^*)$, $Q^* \in \mathcal{O}(n-1)$. If a uniform prior is imposed on Q^*, the posterior density of the structural IRF's is:*

$$\begin{aligned} f(\Theta) = 2^{(n^2-n+2)/2} |C|^{-np} \prod_{i=1}^{n} c_{ii}^{n-i+1} |I_{n-1} + Q^*|^{-(n-2)} \\ |\tilde{D}_{n-1}' (K' \otimes K'C')(I_{n^2} - L_n' L_n)(K \otimes CK) \tilde{D}_{n-1}|^{-1/2} f(B|\Sigma) f(\Sigma) f(s^*). \end{aligned} \tag{29}$$

Proof. As first and major step, one has to take the derivative of $vec(\Theta)$ with respect to $vec(\Phi)'$, $vech(C)'$ and s'. Note that $Q^* = 2(I_{n-1} - S^*)^{-1} - I_{n-1}$ and therefore

$$dQ^* = 2(I_{n-1} - S^*)^{-1} dS (I_{n-1} - S^*)^{-1}. \tag{30}$$

It follows that

$$\begin{aligned} vec(dQ^*) &= 2(((I_{n-1} - S^*)^{-1})' \otimes (I_{n-1} - S^*)^{-1}) vec(dS) \\ &= 2(((I_{n-1} - S^*)^{-1})' \otimes (I_{n-1} - S^*)^{-1}) \tilde{D}_{n-1} ds. \end{aligned} \tag{31}$$

Now comes the step where I depart from Inoue and Kilian (2018). One can express Q as

$$Q = e_1^n (e_1^n)' + KQ^*K'. \tag{32}$$

It follows that

$$\begin{aligned}
d(CQ) &= d(C)Q + Cd(KQ^*K') \\
&= d(C)Q + 2CK(I_{n-1} - S^*)^{-1} dS^* (I_{n-1} - S^*)^{-1} K', &(33)\\
d(\Phi CQ) &= d(\Phi)CQ + \Phi d(C)Q + 2\Phi CK(I_{n-1} - S^*)^{-1} dS^* (I_{n-1} - S^*)^{-1} K', &(34)\\
d(vec(CQ)) &= (Q' \otimes I_n)L_n' d(vech(C)) + 2(I_n \otimes C) vec(K(I_{n-1} - S^*)^{-1} dS^* (I_{n-1} - S^*)^{-1} K') \\
&= (Q' \otimes I_n)L_n' d(vech(C)) + 2(I_n \otimes C) J_Q ds^*, &(35)\\
d\ vec(\Phi CQ) &= (Q'C' \otimes I_{np}) d(vec(\Phi)) + (Q' \otimes \Phi)L_n' d(vech(C)) + (I_n \otimes \Phi C) J_Q ds^*, &(36)
\end{aligned}$$

where $J_Q := (K((I_{n-1} - S^*)^{-1})' \otimes K(I_{n-1} - S^*)^{-1})\tilde{D}_{n-1}$.
Remembering that $\Theta = [(CQ)'\ (\Phi CQ)']'$ it follows from (35) and (36) that

$$J_1 := \frac{\partial vec(\Theta)}{\partial [vech(C)'\ (s^*)'\ vec(\Phi)]} = \begin{bmatrix} (Q' \otimes I_n)L_n' & (I_n \otimes C)J_Q & 0_{n^2 \times n^2 p} \\ (Q' \otimes \Phi)L_n' & (I_n \otimes \Phi C)J_Q & (Q'C' \otimes I_{np}) \end{bmatrix}. \tag{37}$$

Because this matrix is block lower triangular its determinant is equal to the product of the determinants of the matrices on the diagonal:

$$\begin{aligned}
|J_1| &= |(Q' \otimes I_n)L_n'\ (I_n \otimes C)J_Q||(Q'C' \otimes I_{np})| \\
&= |(Q' \otimes I_n)L_n'\ (I_n \otimes C)J_Q||C|^{np}. &(38)
\end{aligned}$$

Now one can re-write

$$[(Q' \otimes I_n)L_n'\ (I_n \otimes C)J_Q] = (Q' \otimes I_n)Z, \tag{39}$$

with

$$\begin{aligned}
Z &= [L_n'\ 2(F \otimes G)\tilde{D}_{n-1}], &(40)\\
F &= QK(I_{n-1} - (S^*)')^{-1} = \frac{1}{2}K(I_{n-1} + Q^*) = K(I_{n-1} - S^*)^{-1}, &(41)\\
G &= CK(I_{n-1} - S^*)^{-1} = CF. &(42)
\end{aligned}$$

As a next step, the following equality can be used:

$$|(Q' \otimes I_n)Z| = |Z| = \sqrt{|Z|^2} = \sqrt{|Z'Z|}. \tag{43}$$

Because of

$$\begin{aligned}
Z'Z &= \begin{bmatrix} L_n \\ 2\tilde{D}_{n-1}'(F' \otimes G') \end{bmatrix} \begin{bmatrix} L_n' & 2(F \otimes G)\tilde{D}_{n-1} \end{bmatrix} \\
&= \begin{bmatrix} I_{n(n+1)/2} & 2L_n(F \otimes G)\tilde{D}_{n-1} \\ 2\tilde{D}_{n-1}'(F' \otimes G')L_n' & 4\tilde{D}_{n-1}'(F' \otimes G')(F \otimes G)\tilde{D}_{n-1} \end{bmatrix} &(44)\\
&=: \begin{bmatrix} \mathcal{A} & \mathcal{B} \\ \mathcal{C} & \mathcal{D} \end{bmatrix}
\end{aligned}$$

the squared determinant of Z can be computed as

$$\begin{aligned}|Z'Z| &= |\mathcal{A}||\mathcal{D} - \mathcal{C}\mathcal{A}^{-1}\mathcal{B}|\\ &= |\mathcal{D} - \mathcal{C}\mathcal{B}|\\ &= |4(\tilde{D}'_{n-1}(F' \otimes G')(I_{n^2} - L'_n L_n)(F \otimes G)\tilde{D}_{n-1})|\\ &= 2^{(n-1)(n-2)}|\tilde{D}'_{n-1}(F' \otimes G')(I_{n^2} - L'_n L_n)(F \otimes G)\tilde{D}_{n-1}|. \end{aligned} \tag{45}$$

Now, I define $F^* = (I_{n-1} - S^*)^{-1}$ and $\tilde{D}^+_{n-1} = (\tilde{D}'_{n-1}\tilde{D}_{n-1})^{-1}\tilde{D}'_{n-1}$. Using a result from Magnus (1988) one can write

$$\begin{aligned}&\tilde{D}'_{n-1}(F' \otimes G')(I_{n^2} - L'_n L_n)(F \otimes G)\tilde{D}_{n-1})\\ =&\tilde{D}'_{n-1}((F^*)' \otimes (F^*)')(K' \otimes K')(I_n \otimes C')(I_{n^2} - L'_n L_n)(I_n \otimes C)(K \otimes K)(F^* \otimes F^*)\tilde{D}_{n-1}\\ =&\mathcal{M}'\tilde{D}'_{n-1}(K' \otimes K')(I_n \otimes C')(I_{n^2} - L'_n L_n)(I_n \otimes C)(K \otimes K)\tilde{D}_{n-1}\mathcal{M}, \end{aligned} \tag{46}$$

where $\mathcal{M} = (\tilde{D}^+_{n-1}(F^* \otimes F^*)\tilde{D}_{n-1})$. Again, using Magnus (1988) this leads to

$$|\mathcal{M}| = |F^*|^{n-2} = |\frac{1}{2}I_{n-1} + Q^*|^{n-2} = 2^{-(n-2)(n-1)}|I_{n-1} + Q^*|^{n-2}. \tag{47}$$

Using (38), (39), (43), (45), (46) and (47) one obtains

$$\begin{aligned}|J_1| &= |C|^{np}|(Q' \otimes I_n)L'_n\ (I_n \otimes C)J_Q|\\ &= |C|^{np}|(Q' \otimes I_n)Z|\\ &= |C|^{np}|Z|\\ &= |C|^{np}2^{(n-1)(n-2)/2}|\tilde{D}'_{n-1}(F' \otimes G')(I_{n^2} - L'_n L_n)(F \otimes G)\tilde{D}_{n-1}|^{1/2}\\ &= |C|^{np}2^{(n-1)(n-2)/2}|\mathcal{M}||\tilde{D}'_{n-1}(K' \otimes K'C')(I_{n^2} - L'_n L_n)(K \otimes CK)\tilde{D}_{n-1}|^{1/2}\\ &= 2^{-(n-1)(n-2)/2}|C|^{np}|I_{n-1} + Q^*|^{n-2}|\tilde{D}'_{n-1}(K' \otimes K'C')(I_{n^2} - L'_n L_n)(K \otimes CK)\tilde{D}_{n-1}|^{1/2}. \end{aligned} \tag{48}$$

For the remaining derivatives the results from Inoue and Kilian (2018) can be used:

$$|J_2| := \left|\frac{\partial vec(\Phi)}{\partial vec(B)'}\right| = 1, \tag{49}$$

$$|J_3| := \left|\frac{\partial vech(\Sigma)}{\partial vech(C)'}\right| = 2^n \prod_{i=1}^{n} c_{ii}^{n-i+1}. \tag{50}$$

As a last step, (26) can be re-written as

$$\begin{aligned}f(\Theta) &= |J_1|^{-1}|J_2||J_3|f(B|\Sigma)f(\Sigma)f(s^*)\\ &= 2^{(n^2-n+2)/2}|C|^{-np}|I_{n-1} + Q^*|^{-(n-2)}\prod_{i=1}^{n} c_{ii}^{n-i+1}\\ &\qquad |\tilde{D}'_{n-1}(K' \otimes K'C')(I_{n^2} - L'_n L_n)(K \otimes CK)\tilde{D}_{n-1}|^{-1/2}f(B|\Sigma)f(\Sigma)f(s^*). \end{aligned}$$

■